Comparison of $^{12}CO_2^+$ and $^{13}CO_2^+$ alignment following photoionization of carbon dioxide

J. A. Guest, M. A. O'Halloran, and R. N. Zare
Department of Chemistry, Stanford University, Stanford, California 94305

(Received 30 March 1984; accepted 16 May 1984)

Fluorescence polarizations of the $\tilde{B}\,^2\Sigma_u^+$–$\tilde{X}\,^2\Pi_g$ ($\lambda \sim 289$ nm) and $\tilde{A}\,^2\Pi_u$–$\tilde{X}\,^2\Pi_g$ ($\lambda > 310$ nm) transitions in $^{12}CO_2^+$ and $^{13}CO_2^+$ are measured following the photoionization of CO_2 at energies ranging from 18.2 to 31 eV. The rotational alignments and channel ratios of the $^{12}CO_2^+$ and $^{13}CO_2^+$ $\tilde{B}\,^2\Sigma_u^+$ state are identical within experimental error and agree well with existing theoretical calculations. Polarizations for the $\tilde{A}$–$\tilde{X}$ emission differ for $^{12}CO_2^+$ and $^{13}CO_2^+$. We present evidence that this behavior can be explained by considering the influence of the extensive perturbations in the $\tilde{A}$ and $\tilde{B}$ states of the $^{12}CO_2^+$ photoion. Mixed ($\tilde{A}$, $\tilde{B}$) states in $^{12}CO_2^+$ give rise to red-shifted emission ($\lambda > 310$ nm) with a quantum yield $\Phi^{B,A}$ defined as the fraction of red-shifted emission to all emission originating at the $\tilde{B}$ state energy. Using the present alignment data and published $^{12}CO_2^+$ $\tilde{A}$ and $\tilde{B}$ state fluorescence cross sections, $\Phi^{B,A}$ is determined to be nearly independent of ionizing energy with a value of 0.36 at 21.0 eV, in good agreement with other quantum yield measurements.

I. INTRODUCTION

Fluorescence polarization measurements of photoion alignment can provide useful dynamical information on the photoionization of atomic and molecular systems.[1–5] From these alignments, we can extract ratios of partial cross sections for photoelectron ejection into degenerate continuum channels.[6,7] These channel ratios can then be compared to theoretical cross section calculations to test the current understanding of photoelectron ejection dynamics.

The occupied molecular orbitals of CO_2 $\tilde{X}\,^1\Sigma_g^+$ are $(1\sigma_g)^2(1\sigma_u)^2(2\sigma_g)^2(3\sigma_g)^2(2\sigma_u)^2(4\sigma_g)^2(3\sigma_u)^2(1\pi_u)^4(1\pi_g)^4$. Upon irradiation at sufficiently high energy, inner valence electrons are ejected, leaving the molecular ion in an excited electronic state. Thus, at photon energies greater than 17.36 eV, removal of an electron from the $1\pi_u$ orbital produces the CO_2^+ $\tilde{A}\,^2\Pi_u$ state. At photon energies greater than 18.08 eV a new channel opens, with the removal of an electron from the $3\sigma_u$ orbital to form the CO_2^+ $\tilde{B}\,^2\Sigma_u^+$ state.[8–10] Photoelectron angular distributions, described by the β parameter, have been measured for the $1\pi_u$ and $3\sigma_u$ orbitals.[11] Agreement with theoretical calculations for β using the multiple scattering method[12,13] and frozen-core Hartree–Fock method[14] is good.

Poliakoff *et al.*[15] have previously studied autoionizing structure in CO_2 below 18 eV via polarization of the $^{12}CO_2^+$ $\tilde{A}\,^2\Pi_u$–$\tilde{X}\,^2\Pi_g$ fluorescence. We have extended the $^{12}CO_2^+$ $\tilde{A}$–$\tilde{X}$ fluorescence polarization measurements up to 31.0 eV using a synchrotron radiation continuum light source, and we have performed the same studies on $^{13}CO_2^+$ from 18.2 to 31.0 eV. The CO_2^+ $\tilde{B}\,^2\Sigma_u^+$–$\tilde{X}\,^2\Pi_g$ fluorescence polarizations for both $^{12}CO_2$ and $^{13}CO_2$ photoionization have also been measured in the range 18.2–31.0 eV. The primary goal in the analysis of the present measurements is to obtain alignments of the "pure" Born–Oppenheimer $\tilde{A}$ and $\tilde{B}$ states of the CO_2^+ photoion as a function of the ionizing energy. The $\tilde{A}$ and $\tilde{B}$ alignments can be extracted from fluorescence polarizations provided that the spectroscopy of the $\tilde{A}$–$\tilde{X}$ and $\tilde{B}$–$\tilde{X}$ band systems is well understood.[5] The $^{12}CO_2^+$ $\tilde{B}$(000) state, which accounts for most of the $\tilde{B}$ state population in photoionization, is now known to be strongly perturbed by the $\tilde{A}$ state.[16–18] However, in $^{13}CO_2^+$ the $\tilde{B}$(000) level is essentially unperturbed by the $\tilde{A}$ state.[19]

The importance of the $^{12}CO_2^+$ perturbation in interpreting the results of various photoionization studies has not always been recognized. Widely differing values of the apparent $^{12}CO_2^+$ $\tilde{A}/\tilde{B}$ production branching ratio have been determined by a variety of experimental techniques.[18] At an excitation energy of 21.2 eV, the $\tilde{A}/\tilde{B}$ branching ratio was found from photoelectron spectroscopy (PES) to be about 0.65.[20] Resolved fluorescence spectra yielded a value of about 2.7 for the same ratio,[21] and a photon–photoion coincidence technique measured an $\tilde{A}/\tilde{B}$ ratio of about 2.2.[22] Recent electron–photon coincidence studies verify that 0.34 of the $^{12}CO_2^+$ that is supposed to be formed energetically in the $\tilde{B}$ state actually fluoresces in the long-wavelength region generally ascribed to $\tilde{A}$–$\tilde{X}$ emission.[23] Photoelectron and photoion fluorescence branching ratio studies on $^{12}CO_2$, $^{13}CO_2$, and $C^{18}O_2$ show the fluorescence to be isotope dependent, in general accord with predictions from spectroscopic perturbations, while the relative photoelectron branching ratios are isotope independent.[22] Various photoionization models have been proposed to account for the branching ratio discrepancy in CO_2.[14,18,20,24,25] Johnson *et al.*[18] have recently demonstrated through high-resolution fluorescence spectroscopy and quantum yield measurements that $^{12}CO_2^+$ $\tilde{B}$(000) is highly perturbed by the $\tilde{A}$ state, resulting in a significant fraction (0.42) of red-shifted emission in the $\tilde{A}$–$\tilde{X}$ region ($\lambda > 300$ nm). Johnson *et al.* concluded that perturbations between the $\tilde{A}$ and $\tilde{B}$ states were sufficient to account for the $\tilde{A}/\tilde{B}$ branching ratio discrepancy involving the $\tilde{B}$(000) state at an excitation energy of 21.2 eV, but not necessarily the entire $\tilde{A}/\tilde{B}$ branching ratio discrepancy.

It is clear from the above discussion that the extensive CO_2^+ photoion perturbations hinder the direct extraction of

pure $\tilde{A}$ and $\tilde{B}$ alignments. Alignments determined directly from polarizations of the broadband CO_2^+ fluorescence may contain significant contributions from perturbed levels. We address the problem of the effect of photoion perturbations on the measured alignments by invoking reasonable models for CO_2 photoionization. The connection of the $^{12}CO_2^+$ alignment to the $^{13}CO_2^+$ alignment makes it possible for us to evaluate the partial channel ratios for photoejection of the $1\pi_u$ and $3\sigma_u$ electrons from CO_2. These experimental channel ratios are then compared to the theoretical calculations of Padial *et al.*[26]

II. EXPERIMENTAL

The experimental arrangement has been described previously.[5] Gaseous $^{12}CO_2$ (99.9%), supplied by Liquid Carbonic, was made to flow slowly through the sample chamber, which was maintained at a pressure of 5–10 mTorr. Static gas samples of $^{13}CO_2$, supplied by Merck Sharpe and Dohme (90 at. %), were also used. Samples were not purified further. The remaining 10% of isotopes other than $^{13}CO_2$ would not be expected to have any significant effect on the results of the present experiment.

The low-pressure gas samples were photoionized with continuously tunable vacuum ultraviolet synchrotron radiation in the range of 18.2–31 eV (8° beam line at the Stanford Synchrotron Radiation Laboratory). Four focusing mirrors on the beam line assembly enhanced the incident light polarization in the horizontal plane to greater than 97%.[27] Fluorescence from photoions was detected perpendicular to both the propagation direction and the polarization vector of the ionizing radiation. Fluorescence polarization was measured as a function of excitation energy using a photoelastic modulator (PEM) and a crystal polarizer, with optical filters to isolate emission from selected electronic states.

Raw polarizations were corrected for the finite PEM sampling gate width of 2 μs, which is 10% of the total 2π oscillation of the PEM crystal retardance when the crystal is oscillating at 50 kHz.[5] Effects from the variation in PEM response over the finite bandwidth of the detected emission were found to be small (see Sec. III A).

The systematic polarization bias was checked by (i) remeasuring the N_2^+ $B\,^2\Sigma_u^+$–$X\,^2\Sigma_g^+$ fluorescence polarization two of the authors reported in 1983[5] at selected wavelengths and (ii) measuring the polarization through the fluorescence collection optics of a nominally unpolarized light source placed at the interaction region. The main systematic bias was caused by the variations in counter response to the short gating pulses that were synchronized with the different phases of the PEM oscillation.

Photoion fluorescence excitation spectra were also collected as a function of incident energy and stored on a microcomputer. These were used to check the identity of the fluorescing species.

III. RESULTS AND DISCUSSION

A. $^{12}CO_2^+$ and $^{13}CO_2^+$ $\tilde{A}$–$\tilde{X}$ fluorescence polarization

Figures 1 and 2 show $^{12}CO_2$ and $^{13}CO_2$ results, respectively. The (a) portion of each figure shows the polarization

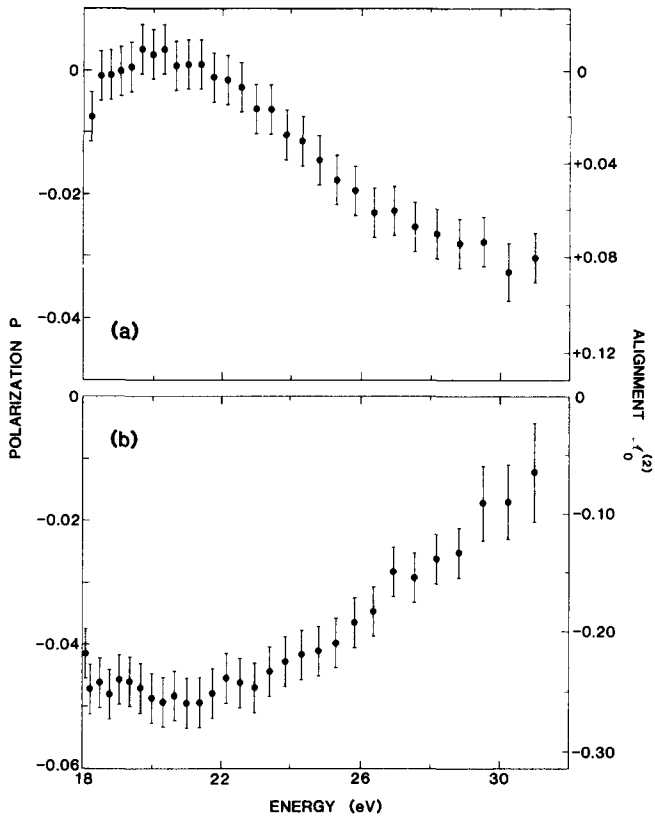

FIG. 1. (a) Degree of polarization P of the $^{12}CO_2^+$ emission of $\lambda > 310$ nm (nominally $\tilde{A}$–$\tilde{X}$) and alignment $\mathscr{A}_0^{(2)}$ of the $^{12}CO_2^+$ photoion following photoionization of $^{12}CO_2$ by a beam of linearly polarized radiation as a function of energy. (b) Degree of polarization P of the $^{12}CO_2^+$ $\tilde{B}$–$\tilde{X}$ emission and alignment $\mathscr{A}_0^{(2)}$ of $^{12}CO_2^+$ $\tilde{B}$ following photoionization of CO_2 by a beam of linearly polarized radiation as a function of energy. All data are taken at 0.90 nm (0.24–0.70 eV) resolution and the error bars represent 2 SD in the photon counting statistics.

of the $^{12}CO_2^+$ and $^{13}CO_2^+$ fluorescence detected in the wavelength region usually assigned to the $\tilde{A}\,^2\Pi_u$–$\tilde{X}\,^2\Pi_g$ transition following photoionization of the CO_2 isotopes. The polarization is plotted as a function of ionizing energy at 0.90 nm (0.24–0.70 eV) resolution. A Corning 7-51 filter, with or without a 0-54 filter, was used to isolate a band of $\tilde{A}$–$\tilde{X}$ fluorescence from the intense $\tilde{B}$–$\tilde{X}$ emission occurring at wavelengths below 300 nm. The error bars in the figures represent two standard deviations (SD) in photon counting statistics, and the polarizations are accurate on an absolute scale to ± 0.01.

The $^{12}CO_2$ was flowed slowly through the cell at a pressure of 5–10 mTorr. The $^{13}CO_2$ measurements were normally made using a static gas sample with replacement every 3–5 h, and polarizations were measured at selected energies using a flowing gas sample. The polarization of $^{12}CO_2^+$ fluorescence was also measured at selected excitation energies using a static gas sample. No difference was found between the polarizations measured using either method for either isotope. The polarizations were found to be independent of pressure over the range of 2–12 mTorr.

Fluorescence polarizations of $^{12}CO_2^+$ were additionally measured through an interference filter centered at 325 nm (12 nm FWHM) which isolated emission from the $^{12}CO_2^+$

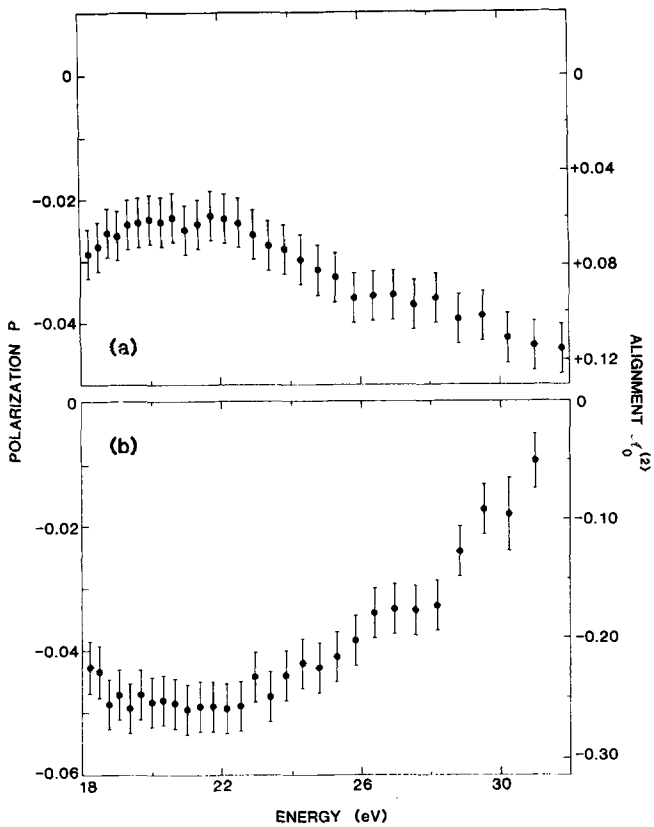

FIG. 2. (a) Degree of polarization P of the $^{13}CO_2^+$ emission at $\lambda > 310$ nm (nominally $\tilde{A}$–$\tilde{X}$) and alignment $\mathscr{A}_0^{(2)}$ of the $^{13}CO_2^+$ photoion following photoionization of $^{13}CO_2$ by a beam of linearly polarized radiation as a function of energy. (b) Degree of polarization P of the $^{13}CO_2^+$ $\tilde{B}$–$\tilde{X}$ emission and alignment $\mathscr{A}_0^{(2)}$ of $^{13}CO_2^+$ $\tilde{B}$ following photoionization of $^{13}CO_2$ by a beam of linearly polarized radiation as a function of energy. All data are taken at 0.90 nm (0.24–0.70 eV) resolution and the error bars represent 2 SD in the photon counting statistics.

$(n+2,0,0)$–$(n,0,0)$ bands.[28] These polarizations were, within the error limits, identical to those measured for the broadband $^{12}CO_2^+$ emission.

It was necessary to consider the effect of variation in PEM response over the relatively large bandwidth of the detected $\tilde{A}$–$\tilde{X}$ fluorescence. The magnitude of this effect was determined by converting the observed polarization to a polarization anisotropy and calculating the correction to the polarization anisotropy at the central wavelength of each of the vibrational bands in the emission.[5] The corrected anisotropies were then weighted by the relative integrated intensities[21] they would have when observed through the filter and averaged. This bandwidth correction was found to be negligibly small. Depolarization by ambient magnetic fields[29] is determined to be negligible in this case, since the $\tilde{A}$ state lifetime is relatively short (~ 120 ns),[23] and the rotational distribution is expected to peak at a high value of N' (~ 15).

B. $^{12}CO_2^+$ and $^{13}CO_2^+$ $\tilde{B}$–$\tilde{X}$ fluorescence polarization

Figures 1(b) and 2(b) show the polarization of the $\tilde{B}\,^2\Sigma_u^+$–$\tilde{X}\,^2\Pi_g$ fluorescence from $^{12}CO_2^+$ and $^{13}CO_2^+$, respectively, following photoionization of the CO_2 isotopes as a function of excitation energy at 0.90 nm (0.24–0.70 eV) resolution. An interference filter centered at 289 nm (10 nm FWHM) isolated the $\tilde{B}$ (000)–$\tilde{X}$ fluorescence from the longer wavelength $\tilde{A}$–$\tilde{X}$ emission. The gas pressures and conditions were as described above. The corrections made to the $\tilde{B}$–$\tilde{X}$ polarizations were the same as those for the $\tilde{A}$–$\tilde{X}$ polarizations. The narrow (~ 10 nm) bandwidth of the $\tilde{B}$–$\tilde{X}$ emission detected through the filter made a PEM wavelength correction unnecessary. Depolarization by ambient magnetic fields was determined to be negligible for the $\tilde{B}$ state, which has a lifetime of $\sim 138 \pm 10$ ns.[18,23] The error bars shown in Figs. 1(b) and 2(b) once again represent 2 SD in photon counting statistics, and the polarizations are accurate on an absolute scale to ± 0.01.

It should be noted that the CO_2^+ $\tilde{C}\,^2\Sigma_g^+$ state, which is produced at ionizing energies greater than 19.39 eV, does not affect the present measurements: since it is fully predissociated, it does not fluoresce to the $\tilde{A}$ or $\tilde{B}$ states.[30]

C. Extraction of the photoion alignment and the channel ratio γ

Because of spectroscopic complications in the CO_2^+ $\tilde{A}$–$\tilde{X}$ and $\tilde{B}$–$\tilde{X}$ emissions, the fluorescence polarizations presented in Figs. 1 and 2 cannot be converted unambiguously to photoion alignments for separable electronic states. Instead, we must postulate models based on available experimental information and try to extract reasonable $\tilde{A}$ and $\tilde{B}$ state alignments using these suppositions.

As a first step in the analysis, we describe a method for determining the CO_2^+ $\tilde{A}$ and $\tilde{B}$ state alignments in the absence of perturbations. The quadrupole alignment $\mathscr{A}_0^{(2)}(N')$ for photoion rotational level N' is described by the relation[5,7]

$$\mathscr{A}_0^{(2)}(N') = \frac{1}{h^{(2)}(N', N'')} \frac{4P}{3-P}, \tag{1}$$

where the geometrical factor $h^{(2)}(N',N'')$ accounts for the effect of the final state N'' on the polarization of the $N' \rightarrow N''$ transition. In the ground state of room temperature CO_2, the most probable value of the nuclear rotation N_0 is 16. Upon photoionization, CO_2^+ $\tilde{A}$ and $\tilde{B}$ states are produced with rotational distributions that do not differ significantly from that of the CO_2 parent. Consequently, the range of populated N' values in CO_2^+ is sufficiently high that fluorescence depolarization due to the effects of isotropic nuclear and electron spin angular momenta is negligible.[5,31] It is reasonable in this case to express the quadrupole alignment in the high-J limit, where

$$\mathscr{A}_0^{(2)} = \frac{4P}{3-P} \tag{2a}$$

for a Q branch ($\Delta J = 0$) and

$$\mathscr{A}_0^{(2)} = \frac{-8P}{3-P} \tag{2b}$$

for a P or R branch ($\Delta J = \pm 1$). The CO_2^+ $\tilde{A} - \tilde{X}$ band can be treated as a Π–Π band system, which at high rotational quantum numbers has intensity only in the members of the P and R branches. The $\tilde{A}$ state alignment is thus determined by

$$\langle \mathscr{A}_0^{(2)}(\tilde{A}) \rangle = \frac{-8P}{3-P}. \tag{3a}$$

At high values of the rotational quantum number, CO_2^+

$\tilde{B}(000)$–$\tilde{X}$ emission can be treated as a quasidiatomic Σ–Π system, where the sum of the intensities of the P and R branches is equal to that for the Q branch.[32] The geometrical factors $h^{(2)}(N',N'')$ are averaged accordingly. Hence, we determine the $\tilde{B}$ state alignment by

$$\langle \mathscr{A}_0^{(2)}(\tilde{B}) \rangle = \frac{16P}{3-P}. \tag{3b}$$

The photoion alignments for $^{12}CO_2^+$ and $^{13}CO_2^+$ determined from Eqs. (3a) and (3b) are shown in Figs. 1 and 2.

Once the quadrupole alignment is found from polarization measurements, it is possible to determine ratios of dynamical photoionization channel amplitudes from $\mathscr{A}_0^{(2)}$. As outlined by Guest, Jackson, and Zare,[5] at high rotation the alignment $\mathscr{A}_0^{(2)}$ can be expressed as

$$\mathscr{A}_0^{(2)} \simeq \tfrac{1}{5}\{4\mathscr{S}_0 - 2(\mathscr{S}_+ + \mathscr{S}_-)\}, \tag{4}$$

where the $\mathscr{S}_i$ are the normalized angular momentum transfer channel probabilities.[33,34] The channel ratio γ, where

$$\gamma = \mathscr{S}_0/(\mathscr{S}_+ + \mathscr{S}_-), \tag{5}$$

can be expressed in terms of the alignment by

$$\gamma = [(2 + 5\,\mathscr{A}_0^{(2)})/(4 - 5\,\mathscr{A}_0^{(2)})]. \tag{6}$$

The value of γ represents the ratio of parity-unfavored to parity-favored[6,7] contributions to the total photoionization cross section. Figures 3 and 4 present the channel ratio γ as a function of ionizing energy for $^{12}CO_2$ and $^{13}CO_2$, respectively. Examination of Figs. 1–4 reveals that the alignments and the channel ratios are effectively identical in both isotopes for the production of the CO_2^+ $\tilde{B}$ state, but that $\mathscr{A}_0^{(2)}$ and γ differ significantly for the CO_2^+ $\tilde{A}$ state.

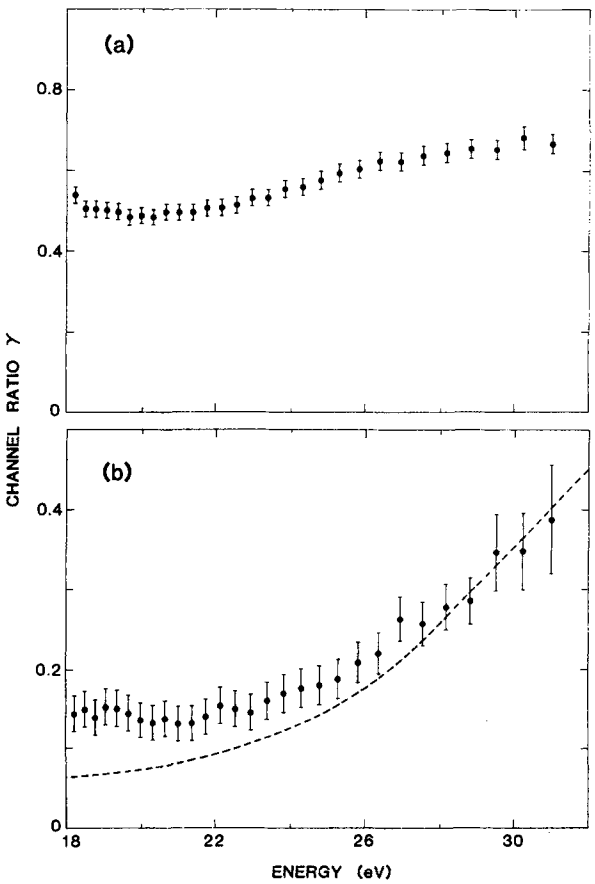

FIG. 3. (a) Plot of the channel ratio γ vs energy of the ionizing radiation for the photoionization of $^{12}CO_2$ leading to photoion emission at $\lambda > 310$ nm ($\tilde{A}$–$\tilde{X}$ region). (b) Plot of the channel ratio γ vs energy of the ionizing radiation for the photoionization of $^{12}CO_2$ leading to CO_2^+ $\tilde{B}$. Dashed curve is from the calculation of Padial *et al.* (Ref. 26). Error bars for all data represent 2 SD.

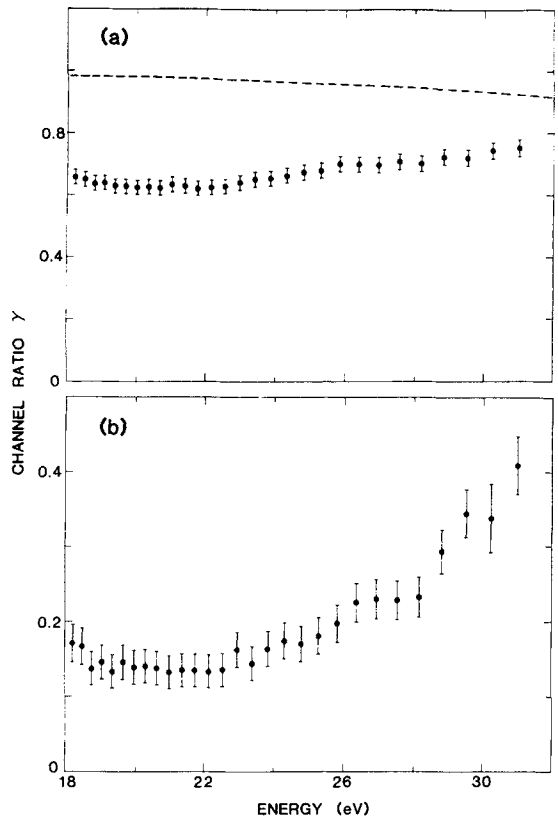

FIG. 4. (a) Plot of the channel ratio γ vs energy of the ionizing radiation for the photoionization of $^{13}CO_2$ leading to photoion emission at $\lambda > 310$ nm ($\tilde{A}$–$\tilde{X}$ region). Dashed curve is from the calculation of Padial *et al.* (Ref. 26). (b) Plot of the channel ratio γ vs energy of the ionizing radiation for the photoionization of $^{13}CO_2$ leading to $^{13}CO_2^+$ $\tilde{B}$. Error bars for all data represent 2 SD.

D. Interpretation of the alignment differences

The isotopic substitution of ^{13}C for ^{12}C in CO_2 is not expected to make a noticeable change in the continuum photoionization dynamics as a function of energy. We therefore look for an explanation of the alignment differences in terms of the known perturbations in the final $\tilde{A}$ and $\tilde{B}$ states of the photoion. We consider a model (see Fig. 5)[18,24] where some of the photoions are produced in unperturbed levels of the $\tilde{A}$ and $\tilde{B}$ states (and nonfluorescing states). The rest of the CO_2^+ product is formed in a mixed state, which is described by the wave function $|\psi_m\rangle = C_A|\psi_A\rangle + C_B|\psi_B\rangle$. Because the vibrational overlap with the $\tilde{B}$ part of the mixed wave function from CO_2 $\tilde{X}(000)$ is good and the overlap to the levels of $\tilde{A}$ that mix with $\tilde{B}$ is poor, photoionization to the mixed state proceeds largely through a $3\sigma_u$-type electron ejection. Therefore *the mixed state photoions should be aligned as if they were formed in a pure $\tilde{B}$ state.* The distribution of fluorescence from the mixed state is determined by its Franck–Condon overlap with the CO_2^+ $\tilde{X}\,^2\Pi_g$ ground state. This overlap is such that only the $\tilde{B}\,^2\Sigma_u^+$ part of the mixed state

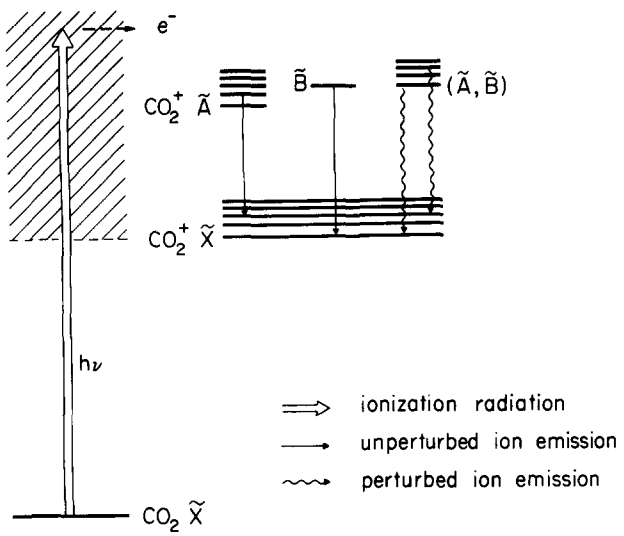

FIG. 5. $^{12}CO_2$ photoionization model used in the data analysis (see Refs. 18 and 24). Photoionization leads to unperturbed levels of the $^{12}CO_2^+$ $\tilde{A}$ and $\tilde{B}$ state and a mixed state resulting from interelectronic coupling of $\tilde{A}$ and $\tilde{B}$.

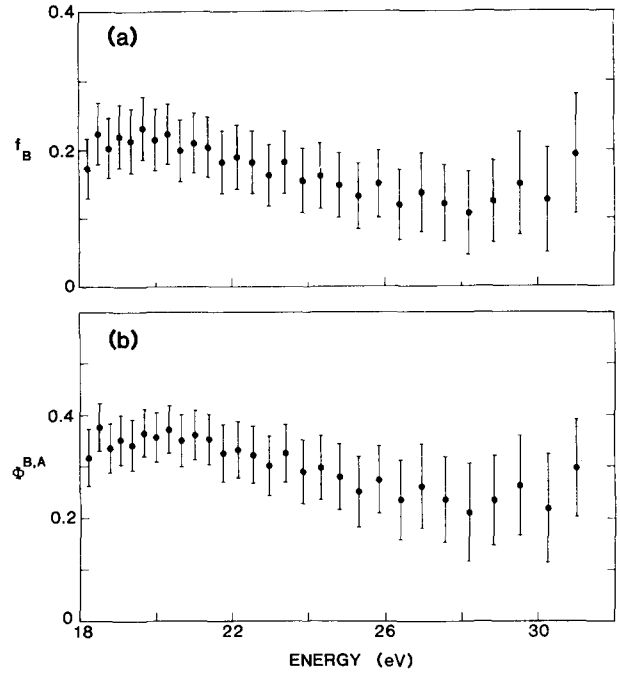

FIG. 6. (a) Plot of f_B, the ratio of emission from the mixed state in the $\tilde{A}$–$\tilde{X}$ manifold to the total emission in the $\tilde{A}$–$\tilde{X}$ region, for $^{12}CO_2^+$ as determined from the alignment data using Eq. (7). (b) Plot of the quantum yield $\Phi^{B,A}$ for apparent $\tilde{B}$ state emission in the $\tilde{A}$–$\tilde{X}$ region. Error bars for both plots represent 2 SD determined from uncertainties in the polarization measurements.

fluoresces to the $\tilde{X}\,^2\Pi_g$ state in the 290 nm region, while only the $\tilde{A}\,^2\Pi_u$ part of the mixed state emits photons at wavelengths greater than 310 nm. Cross terms are expected to make a negligible contribution to the fluorescence transition probabilities because emission from the two electronic states are so well separated in frequency.

Recall that $\tilde{B}$ (000) in $^{13}CO_2^+$ is unperturbed and $\tilde{B}$ (000) in $^{12}CO_2^+$ is heavily perturbed by the $\tilde{A}$ state. Thus the observed $\tilde{B}$ state alignments in both isotopes are effectively identical because the oscillator strength for photoionization to the mixed state in $^{12}CO_2^+$ is carried by the $\tilde{B}$ part of the wave function, and the alignment of the mixed state will be that of the $\tilde{B}$ state. The portion of the mixed state that fluoresces in the $\tilde{A}$ manifold in $^{12}CO_2^+$ will also have the alignment of a pure $\tilde{B}$ state. This alignment is of opposite sign to that of the nearly unperturbed $\tilde{A}$ state in $^{13}CO_2^+$ [cf. Figs. 1(b) and 2(a)]. Therefore, the observed $\tilde{A}$ state alignment in $^{12}CO_2^+$ is expected to be smaller in magnitude than that for the pure $\tilde{A}$ state. This is what is observed [cf. Fig. 1(a) with Fig. 2(a)].

We quantify the results of the model presented in Fig. 5 by supposing that (i) the alignment measured for the $\tilde{B}$ state of both isotopes represents the alignment of the unperturbed $\tilde{B}$ state and (ii) the alignment measured for the $\tilde{A}$ state of $^{13}CO_2^+$ represents the alignment of the unperturbed $\tilde{A}$ state. This is a good assumption provided that most of the $^{13}CO_2^+$ $\tilde{B}$ state is produced in the unperturbed (000) level. Then the measured alignment for $^{12}CO_2^+$ $\tilde{A}$ from fluorescence polarizations in the "$\tilde{A}$–$\tilde{X}$" region $\langle \mathscr{A}_0^{(2)}(^{12}CO_2^+\,\tilde{A})\rangle$ can be expressed as a population-weighted average of the $^{13}CO_2^+$ $\tilde{A}$ and the $^{12}CO_2$ (or $^{13}CO_2$) $\tilde{B}$ alignments

$$\langle \mathscr{A}_0^{(2)}(^{12}CO_2^+\,\tilde{A})\rangle = f_B\langle \mathscr{A}_0^{(2)}(CO_2^+\,\tilde{B})\rangle + (1-f_B)\langle \mathscr{A}_0^{(2)}(^{13}CO_2^+\,\tilde{A})\rangle\,, \quad (7)$$

where f_B is the fraction of the emission in the $\tilde{A}$–$\tilde{X}$ region that is from the mixed state. Figure 6(a) plots f_B vs ionizing energy. The error bars represent 2 SD of the uncertainty in the polarization measurements.

If we know the $\tilde{A}/\tilde{B}$ fluorescence branching ratio as a function of ionizing energy, then we can use the values of Fig. 6(a) to determine an effective quantum yield $\Phi^{B,A}$ for the fraction of the $^{12}CO_2^+$ produced energetically in the $\tilde{B}$ state that will fluoresce in the long-wavelength $\tilde{A}$–$\tilde{X}$ region. This quantum yield is expressed as

$$\Phi^{B,A} = \frac{f_B\sigma_A^{fl}(E)}{\sigma_B^{fl}(E) + f_B\sigma_A^{fl}(E)} \quad (8)$$

at each excitation energy. The values of $\sigma_A^{fl}(E)$ are the $^{12}CO_2^+$ photoion fluorescence cross sections at $\lambda > 310$ nm measured by Lee *et al.*[35] and the values of $\sigma_B^{fl}(E)$ are the $^{12}CO_2^+$ $\tilde{B}$–$\tilde{X}$ photoion fluorescence cross sections in the 289 nm region measured by Carlson *et al.*[36] Calculation of $\Phi^{B,A}$ by this model requires no assumptions other than those made in determining f_B. The quantum yield $\Phi^{B,A}$ determined from Eq. (8) is plotted in Fig. 6(b). Errors are estimated as for Fig. 6(a). The quoted errors in the fluorescence cross sections are not included in the uncertainties.

The quantum yield $\Phi^{B,A}$ in Fig. 6(b) appears to depend only slightly on energy. The nature of the $(\tilde{A},\tilde{B})$ perturbation in the $^{12}CO_2^+$ photoion should not be affected by the ionizing energy. However, the vibrational distribution in the CO_2^+ $\tilde{A}$ and $\tilde{B}$ states could vary as the ionizing energy increases, causing the fraction of mixed levels to change. This could account for the apparent variation that we observe in the quantum yield $\Phi^{B,A}$ with ionizing energy. The present result of 0.36 for $\Phi^{B,A}$ at 21.0 eV agrees quantitatively with experimental quantum yield studies at 21.2 eV.[18]

From the results of Fig. 6, it is clear that the mixing

model diagrammed in Fig. 5 describes the $^{12}CO_2^+$ photoion alignment adequately. We can also approach this problem by assuming that the $^{12}CO_2^+$ and $^{13}CO_2^+$ $\tilde{A}/\tilde{B}$ PES branching ratios of about 0.65[20,22] correctly describe the $\tilde{A}$ and $\tilde{B}$ state production in CO_2^+, insofar as the mixed state is assigned as being produced in the $\tilde{B}$ manifold. Citing the photoionization model of Fig. 5, we suppose that the $\tilde{A}/\tilde{B}$ fluorescence branching ratios of 2.20 ± 0.30 for $^{12}CO_2^+$ and 1.37 ± 0.50 for $^{13}CO_2^+$ photoionization at 21.2 eV[22] differ from the PES results only because of $(\tilde{A},\tilde{B})$ perturbations. The fractions of $^{12}CO_2^+$ and $^{13}CO_2^+$ that are formed in perturbed levels are again assumed to be aligned as the pure $\tilde{B}$ state. The pure $\tilde{A}$ state alignment that is determined from our data using these assumptions gives the physically unrealistic result that the alignment is larger than the high J limiting value of 0.20 for a perpendicular $|\Delta\Lambda| = 1$ transition.[5] Therefore, if the mixing model shown in Fig. 5 is valid, there is an inconsistency between the present alignment measurements and the previously reported PES $\tilde{A}/\tilde{B}$ branching ratios. This may be caused by misassignment of part of the photoelectron spectrum, resulting in a low $\tilde{A}/\tilde{B}$ branching ratio. Such a possibility seems likely because of the low resolution of photoelectron experiments.

We have assumed in our analysis that the perturbed emission in the $\tilde{A}$–$\tilde{X}$ region can be described as a Π–Π transition in the high-J limit. This is not strictly true, because the perturbations are strong in a region of the $\tilde{A}$ state energy levels where several quanta of ν_2 bending must be excited.[17] Renner–Teller interactions will thus complicate the fluorescence from the perturbed state, which is no longer linear. However, small deviations are not expected to be significant.

E. Comparison with theory

Padial *et al.*[26] have provided theoretical partial cross sections for CO_2 photoionization to continuum electron states, which may be compared to our experimentally derived channel ratios. Photoionization of CO_2 to give the $\tilde{B}\,^2\Sigma_u^+$ state of the photoion is described as proceeding through the dipole-allowed ejection of a $3\sigma_u$ electron to the $(\epsilon\sigma_g,\epsilon\pi_g)$ continuum states. This process is exactly analogous to that described previously for N_2 and CO photoionization.[5] The theoretical cross sections of Padial *et al.*[26] are related to our channel ratio γ by[5,37]

$$\gamma = \frac{D_\Pi^2/D_\Sigma^2}{2 + D_\Pi^2/D_\Sigma^2}, \tag{9}$$

where D_Σ^2 is the dipole strength for $3\sigma_u \rightarrow \epsilon\sigma_g$ photoejection and D_Π^2 is the dipole strength for $3\sigma_u \rightarrow \epsilon\pi_g$ photoejection.

CO_2 photoionization to give CO_2^+ $\tilde{A}\,^2\Pi_u$ proceeds through the dipole-allowed ejection of a $1\pi_u$ electron to the $(\epsilon\sigma_g,\epsilon\pi_g,\epsilon\delta_g)$ continuum states. At high J, we describe the absorption as having Σ–Σ or Σ–Π character based on the combined ion core plus photoelectron angular momentum projection along the internuclear axis. The $1\pi_u \rightarrow \epsilon\sigma_g$ and $1\pi_u \rightarrow \epsilon\delta_g$ channels are equivalent to a Σ–Π transition in CO_2, while the $1\pi_u \rightarrow \epsilon\pi_g$ channel is identified with a Σ–Σ type absorption. Even though three separate degenerate photoejection channels exist in the molecular frame, at high J the $1\pi_u \rightarrow \epsilon\sigma_g$ and $1\pi_u \rightarrow \epsilon\delta_g$ channels have the same type of absorption symmetry, and the dipole strength D_Π^2 equals the sum of these two degenerate cross sections. Thus we can determine the ratio D_Π^2/D_Σ^2.

The dashed line in Fig. 4(a) is the theoretical channel ratio γ for CO_2 photoionization to yield CO_2^+ $\tilde{A}\,^2\Pi_u$. From theory the $1\pi_u \rightarrow \epsilon\delta_g$ transition predominates at the energies studied, resulting in a γ very near its maximum possible value of 1. This strong transition is expected to be atomic-like in character ($2p$–ϵd). The $1\pi_u \rightarrow \epsilon\sigma_g$ is weak because of intensity borrowing by $1\pi_u \rightarrow 5\sigma_g$ discrete transitions.[26] The $1\pi_u \rightarrow \epsilon\pi_g$ transition is also weak because it is closely related to a forbidden atomic-like $2p$–ϵp transition.

The experimental channel ratio γ in $^{13}CO_2^+$ for the removal of the $1\pi_u$ electron indicates that the $1\pi_u \rightarrow (\epsilon\delta_g,\epsilon\sigma_g)$ ejections should dominate the dynamics, but not as fully as theory indicates. This lack of quantitative agreement may be caused by neglecting configuration interaction effects, as was the case for $2\sigma_u$ photoejection in N_2.[4,5,38] If $^{13}CO_2^+$ $\tilde{A}$ is not free from perturbations, then our determined alignments may not be attributable to a pure $\tilde{A}$ state.

The theoretical channel ratios for $3\sigma_u$ electron photoejection shown by the dashed line in Fig. 3(b) agree very well with our experiments on $^{12}CO_2^+$ and $^{13}CO_2^+$. Padial *et al.*[26] predict that the $3\sigma_u \rightarrow \epsilon\sigma_g$ cross-section peaks just above threshold because of a low-lying $5\sigma_g$ (σ^*) virtual valence orbital in this region. The $3\sigma_u \rightarrow \epsilon\pi_g$ channel increases slowly with energy and peaks at around 35 eV because of a growing $d\pi$ orbital contribution. These partial cross sections lead to a strongly energy-dependent γ, in agreement with the results of our experiment.

IV. CONCLUSION

Upon photoionization of carbon dioxide at sufficiently high energies, the CO_2^+ ion is produced in the $\tilde{A}$ and $\tilde{B}$ excited states. We have measured the polarization of the unresolved $\tilde{A}$–$\tilde{X}$ and $\tilde{B}$–$\tilde{X}$ fluorescence as a function of ionizing energy (18.2 to 31 eV) for both $^{12}CO_2^+$ and $^{13}CO_2^+$. For $^{13}CO_2^+$, the $\tilde{A}$ and $\tilde{B}$ states are nearly unperturbed and it is a straightforward matter to extract the alignment of the $\tilde{A}$ and $\tilde{B}$ state photoions, which are taken to be those of the pure states. For $^{12}CO_2^+$, the $\tilde{A}$ and $\tilde{B}$ states are strongly mixed.

We interpret the polarization data by invoking a model in which $\tilde{A}$, $\tilde{B}$, and mixed $(\tilde{A},\tilde{B})$ levels are produced and (because of the photoionization Franck–Condon factors) the mixed levels have the alignment of the $\tilde{B}$ state. By assuming the alignments of the $\tilde{A}$ and $\tilde{B}$ states to be the same for $^{12}CO_2^+$ and $^{13}CO_2^+$, we find that the fraction of emission in the $\tilde{A}$–$\tilde{X}$ region originating from the mixed $(\tilde{A},\tilde{B})$ state is about 0.20, nearly independent of ionizing energy. This implies a quantum yield for apparent $\tilde{B}$–$\tilde{X}$ emission in the $\tilde{A}$–$\tilde{X}$ wavelength region of 0.36 ± 0.05 (at 21 eV), in close agreement with other estimates of this quantity. However, our alignment data cannot be reconciled with previously reported $\tilde{A}/\tilde{B}$ photoelectron branching ratios in both $^{12}CO_2^+$ and $^{13}CO_2^+$. Degenerate photoionization channel ratios have been extracted from the alignment data. Comparison with the separated channel static exchange calculations of Padial

et al.[26] shows good agreement of the channel ratios for the removal of a $3\sigma_u$ electron to produce the CO_2^+ $\tilde{B}$ state, but less satisfactory agreement for the removal of a $1\pi_u$ electron to produce the CO_2^+ $\tilde{A}$ state.

ACKNOWLEDGMENTS

We thank Odile Dutuit for helpful experimental assistance. These experiments were performed at the Stanford Synchrotron Radiation Laboratory, which was supported by the U.S. Department of Energy, Office of Basic Energy Sciences, and the National Science Foundation Division of Materials Research. This work was supported by the National Science Foundation under Grant Nos. NSF PHY 79-08694 and NSF PHY 82-06400. RNZ gratefully acknowledges support through the Shell Distinguished Chairs Program, funded by the Shell Companies Foundation, Inc.

[1]C. D. Caldwell and R. N. Zare, Phys. Rev. A **16**, 255 (1977).
[2]W. Kronast, R. Huster, and W. Mehlhorn, J. Phys. B **17**, L51 (1984).
[3]C. D. Caldwell, Z. M. Goodman, and M. G. White, Bull. Am. Phys. Soc. **29**, 798 (1984).
[4]E. D. Poliakoff, J. L. Dehmer, D. Dill, A. C. Parr, K. H. Jackson, and R. N. Zare, Phys. Rev. Lett. **46**, 907 (1981).
[5]J. A. Guest, K. H. Jackson, and R. N. Zare, Phys. Rev. A **28**, 2217 (1983).
[6]C. H. Greene and R. N. Zare, Phys. Rev. A **25**, 2031 (1982).
[7]C. H. Greene and R. N. Zare, Annu. Rev. Phys. Chem. **33**, 119 (1982).
[8]Y. Tanaka and M. Ogawa, Can. J. Phys. **40**, 879 (1962).
[9]C. R. Brundle and D. W. Turner, Int. J. Mass Spectrom. Ion Phys. **2**, 195 (1969).
[10]J. Berkowitz, *Photoabsorption, Photoionization, and Photoelectron Spectroscopy* (Academic, New York, 1979).
[11]F. A. Grimm, J. D. Allen, Jr., T. A. Carlson, M. O. Krause, D. Mehaffy, P. R. Keller, and J. W. Taylor, J. Chem. Phys. **75**, 92 (1981).
[12]F. A. Grimm, T. A. Carlson, W. B. Dress, P. Agron, J. D. Thomson, and J. W. Davenport, J. Chem. Phys. **72**, 3041 (1980).
[13]J. R. Swanson, D. Dill, and J. L. Dehmer, J. Phys. B **14**, L207 (1981).
[14]R. R. Lucchese and V. McKoy, Phys. Rev. A **26**, 1406 (1982).
[15]E. D. Poliakoff, J. L. Dehmer, A. C. Parr, and G. E. Leroi, J. Chem. Phys. **77**, 5243 (1982).
[16]J. Rostas and R. P. Tuckett, J. Mol. Spectrosc. **96**, 77 (1982).
[17]M. A. Johnson, J. Rostas, and R. N. Zare, Chem. Phys. Lett. **92**, 225 (1982).
[18]M. A. Johnson, R. N. Zare, J. Rostas, and S. Leach, J. Chem. Phys. **80**, 2407 (1984).
[19]C. Larcher, Ph.D. thesis, Orsay, France, 1982.
[20]J. A. R. Samson, and J. L. Gardner, J. Geophys. Res. **78**, 3663 (1973).
[21]L. C. Lee and D. L. Judge, J. Chem. Phys. **57**, 4443 (1972).
[22]S. Leach, M. Devoret, and J. H. D. Eland, Chem. Phys. **33**, 113 (1978).
[23]J. P. Maier and F. Thommen, Chem. Phys. **51**, 319 (1980).
[24]S. Leach, P. R. Stannard, and W. M. Gelbart, Mol. Phys. **36**, 1119 (1978).
[25]T. Gustafsson, E. W. Plummer, D. Eastman, and W. Gudat, Phys. Rev. A **17**, 175 (1978).
[26]N. Padial, G. Csanak, B. V. McKoy, and P. W. Langhoff, Phys. Rev. A **23**, 218 (1981).
[27]V. Rehn, A. D. Baer, J. L. Stanford, D. S. Kyser, and V. O. Jones, in *VUV Radiation Physics*, edited by E. E. Koch, R. Haensel, and C. Kunz (Pergamon Vieweg, London, 1974), p. 780.
[28]T. S. Wauchop and H. P. Broida, J. Geophys. Res. **76**, 21 (1971).
[29]A. C. G. Mitchell and M. W. Zemansky, *Resonance Radiation and Excited Atoms* (Cambridge University, London, 1934).
[30]J. H. D. Eland, Int. J. Mass. Spectrom. Ion Phys. **9**, 397 (1972).
[31]J. A. Guest, M. A. O'Halloran, and R. N. Zare, Chem. Phys. Lett. **103**, 261 (1984).
[32]G. Herzberg, *Molecular Spectra and Molecular Structure. I. Spectra of Diatomic Molecules* (Van Nostrand Reinhold, New York, 1950).
[33]U. Fano and D. Dill, Phys. Rev. A **6**, 185 (1972); D. Dill and U. Fano, Phys. Rev. Lett. **29**, 1203 (1972).
[34]S. D. Druger, J. Chem. Phys. **64**, 987 (1976).
[35]L. C. Lee, R. W. Carlson, and D. L. Judge, J. Phys. B **9**, 855 (1976).
[36]R. W. Carlson, D. L. Judge, and M. Ogawa, J. Geophys. Res. **78**, 3194 (1973).
[37]J. L. Dehmer and D. Dill, Phys. Rev. A **18**, 164 (1978).
[38]M. Raoult, H. Le Rouzo, G. Raseev, and H. Lefebvre-Brion, J. Phys. B **16**, 4601 (1983).